

# **$\alpha$ -catenin facilitates mechanosensing and rigidity-dependent growth by linking integrin adhesions to F-actin**

By: Abhishek Mukherjee<sup>1</sup>, Elisabeth Nadjar-Boger<sup>1</sup>, Michael P. Sheetz<sup>2</sup> & Haguy Wolfenson<sup>1,\*</sup>

## **Affiliations**

<sup>1</sup>Department of Genetics and Developmental Biology, Rappaport Faculty of Medicine, Technion – Israel Institute of Technology, Haifa 31096, Israel

<sup>2</sup>Department of Biochemistry and Molecular Biology, University of Texas Medical Branch, Galveston, TX 77555, USA

\*Correspondence to: [haguyw@technion.ac.il](mailto:haguyw@technion.ac.il)

## **Abstract**

The physical interactions of cells with their external environment are critical for their survival and function. These interactions are altered upon epithelial to mesenchymal transition (EMT) as cells switch from relying primarily on cell-cell adhesions to relying on cell-matrix adhesions. Mechanical signals are central to regulating these two types of interactions, but the crosstalk and the mechanobiological processes that mediate the transition between them are poorly understood. Here we show that  $\alpha$ -catenin, a mechanosensitive protein that regulates cadherin-based cell-cell adhesions, directly interacts with integrin adhesions and regulates their growth as well as their transmission of mechanical forces into the matrix. In mesenchymal cells,  $\alpha$ -catenin is recruited to the cell edge where it interacts with actin in regions devoid of  $\alpha$ -actinin. As actin and  $\alpha$ -catenin flow from the cell edge toward the center,  $\alpha$ -catenin interacts with vinculin within integrin adhesions to mediate adhesion maturation, enhance force transmission, and drive the proper assembly of actin stress fibers. Importantly, in the absence of  $\alpha$ -catenin–vinculin interactions, cell adhesion to the matrix is impaired, and the cells display aberrant responses to matrix rigidity which is manifested in rigidity-independent growth. These results provide a novel understanding of  $\alpha$ -catenin as having a dual-role in mechanosensing by both cell-cell and cell-matrix adhesions.

## **Introduction**

The ability of cells to sense and respond to their immediate extracellular environment affects the most fundamental cellular functions, including survival, proliferation, and migration, among others<sup>1-3</sup>. This sensing ability relies on direct physical interactions with neighboring cells and/or with the extracellular matrix (ECM) which are facilitated by cell adhesion molecules – cadherin and integrin, respectively<sup>4</sup>. The balance and transition between these two types of interactions can determine the state of a cell, for example, during the process of epithelial to mesenchymal transition (EMT). However, the mechanisms of interplay between cell-cell and cell-matrix adhesions remain poorly understood.

Cell-cell interactions are classically mediated by adherens junctions (AJs), which are composed of transmembrane E-Cadherin molecules and the catenin family of proteins – including p120-catenin,  $\beta$ -catenin, and  $\alpha$ -catenin – which form complexes that bind to the cytoplasmic tails of the cadherins<sup>5</sup>.  $\alpha$ -catenin is an actin binding protein, and its ability to mediate the connection between cadherin and the actin cytoskeleton is vital for AJs, as actomyosin-based forces are required for stabilizing the cadherin-cadherin connection<sup>6,7</sup>. Myosin II motors that operate on actin filaments create a tension in  $\alpha$ -catenin and cause structural changes in its C-terminal actin-binding domain (ABD), and in its M-domain<sup>8</sup>. The former facilitates binding to filamentous actin (F-actin) bundles, whereas the latter allows the recruitment of other adhesion-related proteins, including vinculin,  $\alpha$ -actinin, ZO-1, formin-1, and afadin<sup>9</sup>. Thus,  $\alpha$ -catenin acts as a mechanosensory protein, i.e., it is activated when forces are applied to it<sup>10,11</sup>. Notably, by competing with the actin polymerization complex Arp2/3 (actin-related protein 2/3) for actin filaments,  $\alpha$ -catenin prevents the formation of dynamic lamellipodia (which are associated with mesenchymal cells) thereby assisting in the maintenance of epithelial integrity<sup>12,13</sup>.

Cell-matrix adhesions, classically referred to as focal adhesions (FAs), connect the ECM to the actin cytoskeleton<sup>14,15</sup>. At the heart of these adhesions are the transmembrane integrins, which bind to the ECM using their large extracellular domains, and to F-actin through a layer of adaptor proteins that bind to their cytoplasmic tails<sup>16</sup>. Notably,  $\alpha$ -actinin and vinculin are  $\alpha$ -catenin binding proteins which are essential FA adaptors that regulate the assembly, growth, and stability of FAs<sup>17</sup>. This might suggest that the  $\alpha$ -catenin/ $\alpha$ -actinin/vinculin module could have a role in the shift in balance between cell-cell and cell-matrix adhesions during EMT. Previous studies have suggested a role for  $\alpha$ -catenin outside of cell-cell adhesions<sup>18-21</sup>, but whether  $\alpha$ -catenin plays a role in regulation of cell-matrix adhesions is unknown.

Here we show that in mesenchymal cells,  $\alpha$ -catenin is recruited to the cell edge where it interacts with actin in regions devoid of  $\alpha$ -actinin. The recruitment process itself is independent of  $\alpha$ -actinin and vinculin, but is enhanced upon activation of cells using epidermal growth factor (EGF), and is more rapid and efficient when cells are plated on stiff matrices compared to soft. Following its recruitment to the cell edge,  $\alpha$ -catenin undergoes retrograde flow together with F-actin towards the center, and then it interacts with vinculin within integrin adhesions. This interaction mediates adhesion maturation, enhances transmission of forces to the matrix, and drives proper assembly of actin stress fibers. Further, we found that while  $\alpha$ -catenin is not necessary for the decision to undergo rigidity-dependent EMT, the absence of the  $\alpha$ -catenin–vinculin interactions leads

mesenchymal cells to have impaired adhesions to the matrix, which results in the aberrant mechanosensing of matrix rigidity, and the transformation of the cells to display rigidity-independence for growth.

## **Results**

### **$\alpha$ -catenin localizes to the cell edge in fibroblasts**

Since  $\alpha$ -catenin was shown to be recruited to the edges of mesenchymal cells<sup>20</sup>, we postulated that it might play a role in regulating integrin adhesions that assemble in these regions. To test this, we first verified the recruitment of  $\alpha$ -catenin to the edge of three different fibroblast cell lines: NIH3T3, human foreskin fibroblasts and RPTP $\alpha^{+/+}$  mouse fibroblasts (which henceforth will be referred to as MEFs). We plated the cells sparsely on coverslips coated with fibronectin (FN) to prevent the formation of cell-cell contacts, and fixed them after 15 minutes of cell spreading. In all cases, immunostaining confirmed the localization of  $\alpha$ -catenin in lamellipodial regions, typically as a narrow stripe (710 $\pm$ 64 nm wide; n=20) in the direction perpendicular to the cell edge (Fig. 1A).

Next, we used MEFs in order to characterize the relationship between  $\alpha$ -catenin and its known binding partners in AJs – F-actin,  $\alpha$ -actinin, and vinculin – since they are all key players in integrin adhesions as well. Notably, the recruitment of  $\alpha$ -catenin to the cell edge was independent of vinculin and  $\alpha$ -actinin as their depletion from the cells did not affect  $\alpha$ -catenin's localization (Supplementary Fig. 1). Co-staining the cells for  $\alpha$ -catenin and F-actin showed that  $\alpha$ -catenin often decorated actin filaments at the cell edge at early stages of cell spreading (Fig. 1B). At later time points (4 hours), in addition to its localization to the cell edge,  $\alpha$ -catenin was very often associated with actin stress fibers (Supplementary Fig. 2).

In the next step, we co-stained the cells for  $\alpha$ -catenin,  $\alpha$ -actinin, and F-actin. As shown in Supplementary Fig. 3, at early times of cell spreading,  $\alpha$ -actinin appeared in nascent adhesion sites but was also recruited to the very edge of the cell where it was co-localized with F-actin, consistent with previous studies<sup>22,23</sup>. However, close examination of high-resolution confocal images showed that  $\alpha$ -catenin and  $\alpha$ -actinin were not co-localized at the cell edge and often showed non-complementary distributions (Fig. 1C). Similarly, at later time points,  $\alpha$ -catenin and  $\alpha$ -actinin were not co-localized on actin stress fibers (Supplementary Fig. 4). Thus,  $\alpha$ -actinin and  $\alpha$ -catenin decorate actin filaments in a non-overlapping manner. We next turned to test the relative localizations of  $\alpha$ -catenin and vinculin. As expected, vinculin was primarily localized within adhesion sites 1-3  $\mu$ m away from the  $\alpha$ -catenin-rich cell edges; however, in a small number of cases, we observed  $\alpha$ -catenin patches that appeared to be extending from the lamellipodia toward vinculin in these adhesions (Fig. 1D). This suggests that  $\alpha$ -catenin may flow from the cell edge toward integrin adhesions, and interact with them transiently.

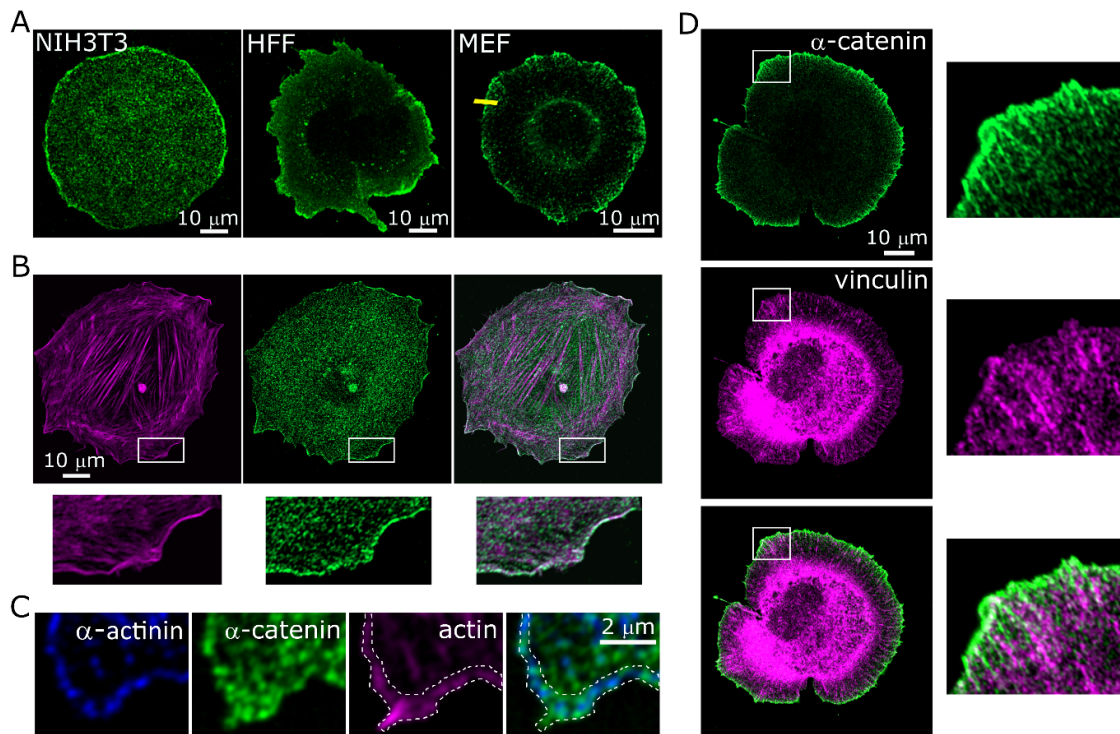


**Figure 1.  $\alpha$ -catenin localizes in the lamellipodium at early times of cell spreading.** A. Representative images of three fibroblast cell lines immunostained for  $\alpha$ -catenin after 15 min of spreading on FN-coated coverslips. B. Co-staining for F-actin (phalloidin) and  $\alpha$ -catenin; bottom panel images are zoom-ins of the boxes in the top images. C. Zoom-in on the edge of a cell co-stained for  $\alpha$ -actinin,  $\alpha$ -catenin, and actin. D. Co-staining for  $\alpha$ -catenin and vinculin; right panel images are zoom-ins of the boxes in the images on the left.

### **$\alpha$ -catenin undergoes retrograde flow with F-actin and interacts with integrin adhesions**

To further explore the relationship between  $\alpha$ -catenin and actin, vinculin and  $\alpha$ -actinin in the context of the lamellipodium and integrin adhesions, we performed live-cell imaging of cells as they attached to FN-coated coverslips. Tracking the dynamics of GFP- $\alpha$ -catenin along with tdTomato-tractin (marker for F-actin<sup>24</sup>) showed that the two markers were predominantly colocalized, and displayed the same protrusion-retraction cycles at the cell edge (Fig. 2A-A', Supplementary Video 1). Moreover,  $\alpha$ -catenin showed the same flow patterns as that of F-actin from the cell edge inwards, and decorated actin stress fibers as they gradually grew over time (Supplementary Video 1). Consistent with the immunostaining results, imaging live cells co-expressing GFP- $\alpha$ -catenin and mCherry- $\alpha$ -actinin showed that they did not overlap (Supplementary Video 2). In particular, during protrusion-retraction cycles, when  $\alpha$ -actinin was associated with the protrusion phase –  $\alpha$ -catenin was associated with the retraction phase, and vice versa (Fig. 2B-B'). Thus, these results imply that  $\alpha$ -catenin and  $\alpha$ -actinin do not interact within the context of cell edge dynamics and integrin adhesions.

In contrast, imaging live cells co-expressing GFP- $\alpha$ -catenin and mCherry-vinculin showed that they had similar dynamics and flow patterns. In particular,  $\alpha$ -catenin co-localized with vinculin within adhesions that were growing and sliding from the cell edge toward the center (Fig. 2C', Supplementary Video 3), suggesting a specific interaction between  $\alpha$ -catenin and maturing FAs. Indeed, temporal averaging of GFP- $\alpha$ -catenin videos revealed patterns of  $\alpha$ -catenin expression that matched the localization of FAs situated 1-3  $\mu$ m back

from the cell edge (Fig. 2C). The fact that these patterns were rarely detected by immunostaining suggests that the apparent interaction between  $\alpha$ -catenin and focal adhesions was transient, which is consistent with the flow of  $\alpha$ -catenin along with F-actin.

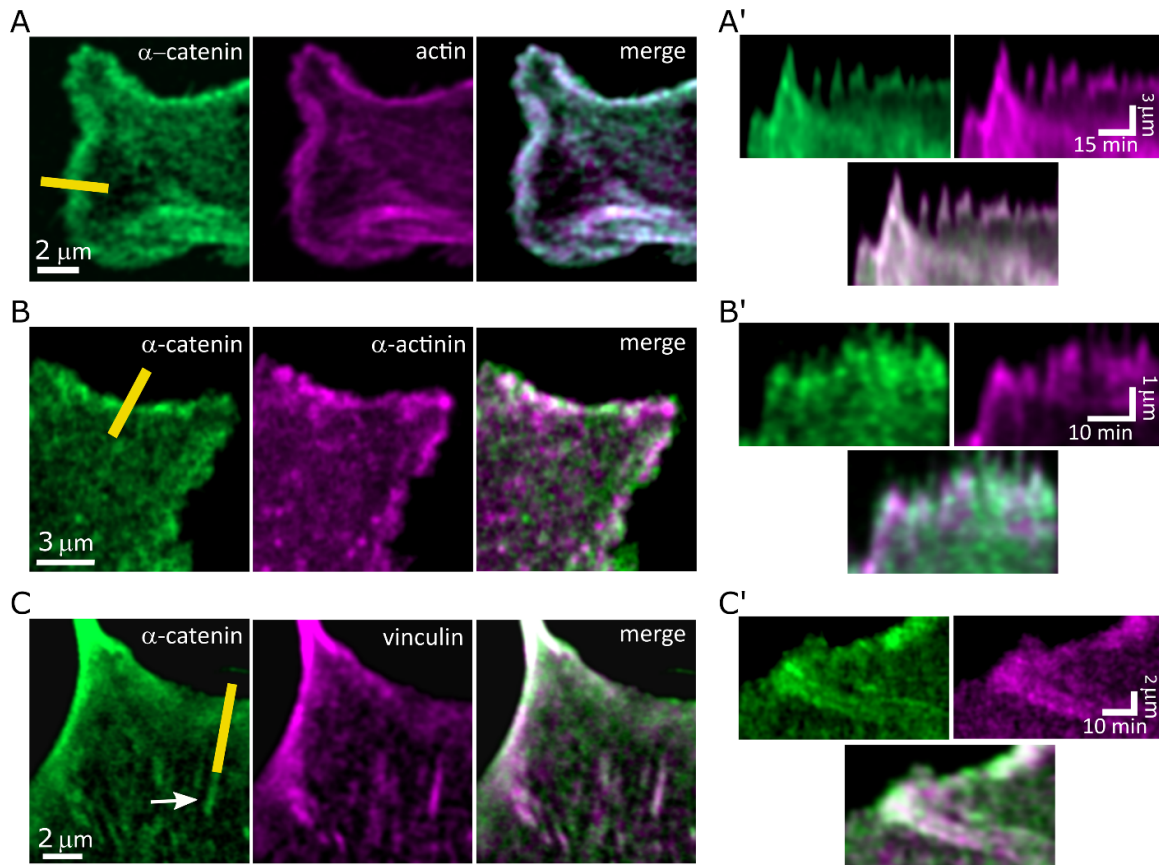


**Figure 2.  $\alpha$ -catenin flows from the cell edge with actin and vinculin.** A. Frame from a movie of a cell expressing GFP- $\alpha$ -catenin and tomato-Tractin showing colocalization of actin and  $\alpha$ -catenin at the edge; A'. Kymographs taken from the yellow line shown in A. B. Frame from a movie of a cell expressing GFP- $\alpha$ -catenin and mCherry- $\alpha$ -actinin showing that two are not colocalized; B'. Kymographs taken from the yellow line shown in B. C. Average of 6 frames (equivalent to 2 min) from a movie of a cell expressing GFP- $\alpha$ -catenin and mCherry-vinculin showing colocalization at the edge as well as in mature adhesions (arrow); C'. Kymographs taken from the yellow line shown in C.

### **$\alpha$ -catenin interacts with vinculin in focal adhesions**

To further explore the interaction between  $\alpha$ -catenin and FAs, we next tested whether a specific connection between  $\alpha$ -catenin and vinculin was the underlying reason for the observed flow patterns of both proteins. To that end, we used a variant of GFP- $\alpha$ -catenin containing a Lysine-to-Proline mutation at site 344 (L344P), which prevents it from binding to vinculin<sup>25,26</sup>. We expressed this variant, along with tdTomato-tractin or mCherry-vinculin, in cells in which the expression level of  $\alpha$ -catenin was knocked-down ( $\alpha$ -catenin KD cells) (Supplementary Fig. 5), and performed live-cell tracking of the cells as they attached to FN-coated coverslips. This revealed stark differences from the aforementioned dynamics observed with wild-type (WT) GFP- $\alpha$ -catenin. First, in many cases, the cells failed to form stable adhesions, and the cell edge displayed extensive ruffling, often separated by rapid bursts of cell edge protrusions (Fig. 3A, Supplementary Video 4). Second,



in cases where less ruffling was observed, the cells failed to form a lamellipodia, and instead they spread by projecting narrow protrusions. However, even though relatively stable vinculin-containing adhesions were present in those protrusions, these adhesions rarely slid towards the cell center, despite the apparent flow of GFP- $\alpha$ -catenin-L344P on top of them (Fig. 3B, Supplementary Video 5). Evidently, the flow rate of GFP- $\alpha$ -catenin-L344P was considerably higher than that of mCherry-vinculin in such adhesions (Fig. 3B, Supplementary Video 5). Third, GFP- $\alpha$ -catenin-L344P often appeared in patches that were moving along actin stress fibers, but unlike cells expressing WT GFP- $\alpha$ -catenin, the stress fibers were highly contractile and more dynamic, leading to the aggregation of GFP- $\alpha$ -catenin-L344P and F-actin at the cell center, near the nucleus (Fig. 3C-D, Supplementary Video 6).

Collectively, these results demonstrate that the  $\alpha$ -catenin–vinculin interaction is necessary for normal cell spreading, regular protrusion/retraction cycles of the cell edge, sliding of integrin adhesions, and proper formation of actin stress fibers.

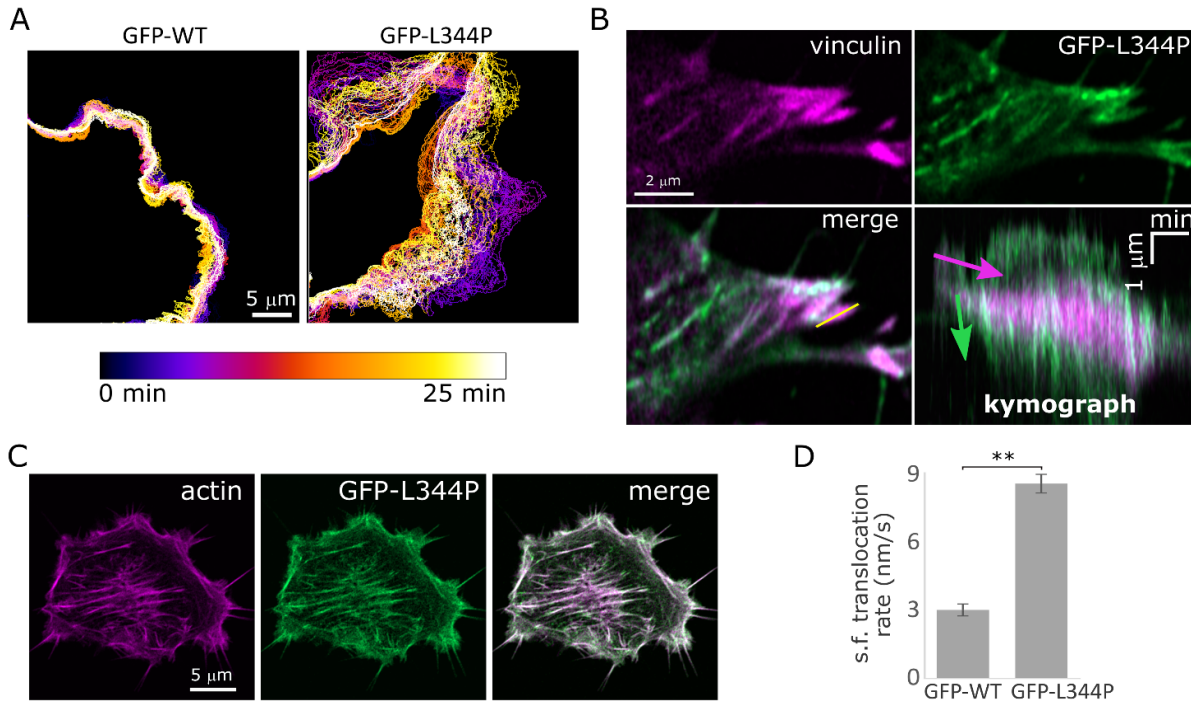


**Figure 3.  $\alpha$ -catenin–vinculin interaction regulates cell edge activity and stress fiber formation.** A. color-coded time-series of the cell edge of  $\alpha$ -catenin KD cells expressing WT GFP- $\alpha$ -catenin (left) and GFP- $\alpha$ -catenin L344P (right), showing much higher cell edge activity in the latter. B. Average of 6 frames (equivalent to 2 min) from a movie zoomed-in on the edge of a cell expressing GFP- $\alpha$ -catenin L344P and mCherry-vinculin; the bottom right image is a kymograph taken from the yellow line shown in the bottom left image. Note the difference in speed (slope) between vinculin (purple arrow) and  $\alpha$ -catenin L344P (green arrow). C. Frames from a movie of a cell expressing GFP- $\alpha$ -catenin L344P and tomato-Tractin showing aggregation of both at the cell center. D. Rate of translocation of stress fibers in cells expressing WT GFP- $\alpha$ -catenin and GFP- $\alpha$ -catenin L344P, as measured from kymographs specifically focused on transverse arc type of stress fibers. N>25; \*\*, P < 0.001 (Student's t-test).

### $\alpha$ -catenin affects focal adhesion maturation and force transmission to the matrix

The results described above indicate that vinculin may act as a clutch that engages with  $\alpha$ -catenin within integrin adhesions as the latter is bound to actin fibers. Indeed, a noticeable disconnect between the flow of  $\alpha$ -

catenin and that of vinculin was observed when the L344P mutation was introduced (compare Fig. 2C and Fig. 3B). Quantification of the flow rates within adhesions showed that the  $\alpha$ -catenin–vinculin interaction attenuated the flow of  $\alpha$ -catenin ~2-fold (Fig. 4A), thus reinforcing the idea that the  $\alpha$ -catenin–vinculin interaction acts as a clutch. Therefore, we next set out to test the effect of this interaction on force transmission to the matrix, as stronger integrin-actin engagement leads to more efficient force transmission. To that end, we plated the cells on arrays of FN-coated pillars and measured the time-dependent deformation of the pillars<sup>27</sup>. As shown in Fig. 4B, WT MEFs gradually displaced the pillars over a period of about 10 min, until reaching a plateau of approximately 120 nm. In agreement with the adhesion maturation results,  $\alpha$ -catenin KD led to a significant decrease in matrix deformation (maximal displacement of ~40 nm). Further, WT-GFP- $\alpha$ -catenin expression restored pillar displacement almost completely (maximal displacement of ~100 nm) whereas GFP- $\alpha$ -catenin-L344P expression did not (Fig. 4B). These results verify that  $\alpha$ -catenin–vinculin binding is a crucial clutch element within adhesions that is required for proper contractile activity and force transmission into the matrix.

Next, we sought to test the effect of the  $\alpha$ -catenin–vinculin interactions on the growth of nascent adhesions into mature FAs, as this process depends on the engagement of the adhesions with the rearward flowing actin cytoskeleton. To that end, we plated cells on FN-coated coverslips for 6 hours and stained them for vinculin and F-actin. Whereas WT MEFs formed mature vinculin-containing FAs,  $\alpha$ -catenin KD cells displayed virtually no mature vinculin-containing adhesions, and displayed almost exclusively small adhesions (‘focal complexes’) at the cell edge (Fig. 4C). Expression of GFP- $\alpha$ -catenin in the  $\alpha$ -catenin KD cells restored the formation of mature FAs, but, importantly, KD cells expressing GFP- $\alpha$ -catenin-L344P displayed similar adhesions as those of  $\alpha$ -catenin KD cells (Fig. 4C). Similar results were obtained when staining for zyxin (Supplementary Fig. 6), a marker for mature FAs<sup>28</sup>, confirming that the observed lack of mature vinculin-containing adhesions was not due to lack of vinculin recruitment into mature adhesions but rather due to the absence of such adhesions all together. Furthermore,  $\alpha$ -catenin KD cells and cells expressing GFP- $\alpha$ -catenin-L344P were significantly smaller than WT cells or cells expressing WT GFP- $\alpha$ -catenin (Fig. 4D), consistent with their inability to form mature adhesions and with their highly contractile stress fibers which, combined together, prevented the cells from spreading normally.

To further test the relevance of the  $\alpha$ -catenin–vinculin interaction in the regulation of integrin adhesions, we used Matrigel (basement membrane like) matrices, which were recently shown to induce the sliding of adhesions from the cell edge toward the center, resulting in highly elongated adhesions near/underneath the nucleus<sup>29</sup>. We plated the cells on Matrigel-coated coverslips, and after overnight incubation we fixed and stained them for vinculin. This revealed that WT MEFs and  $\alpha$ -catenin KD cells expressing WT-GFP- $\alpha$ -catenin formed a significantly higher number of sliding adhesions than the  $\alpha$ -catenin KD cells and  $\alpha$ -catenin KD cells expressing GFP- $\alpha$ -catenin-L344P (Fig. 4E). These results reinforce the notion that the  $\alpha$ -catenin–vinculin interaction plays a critical role in integrin adhesion regulation.

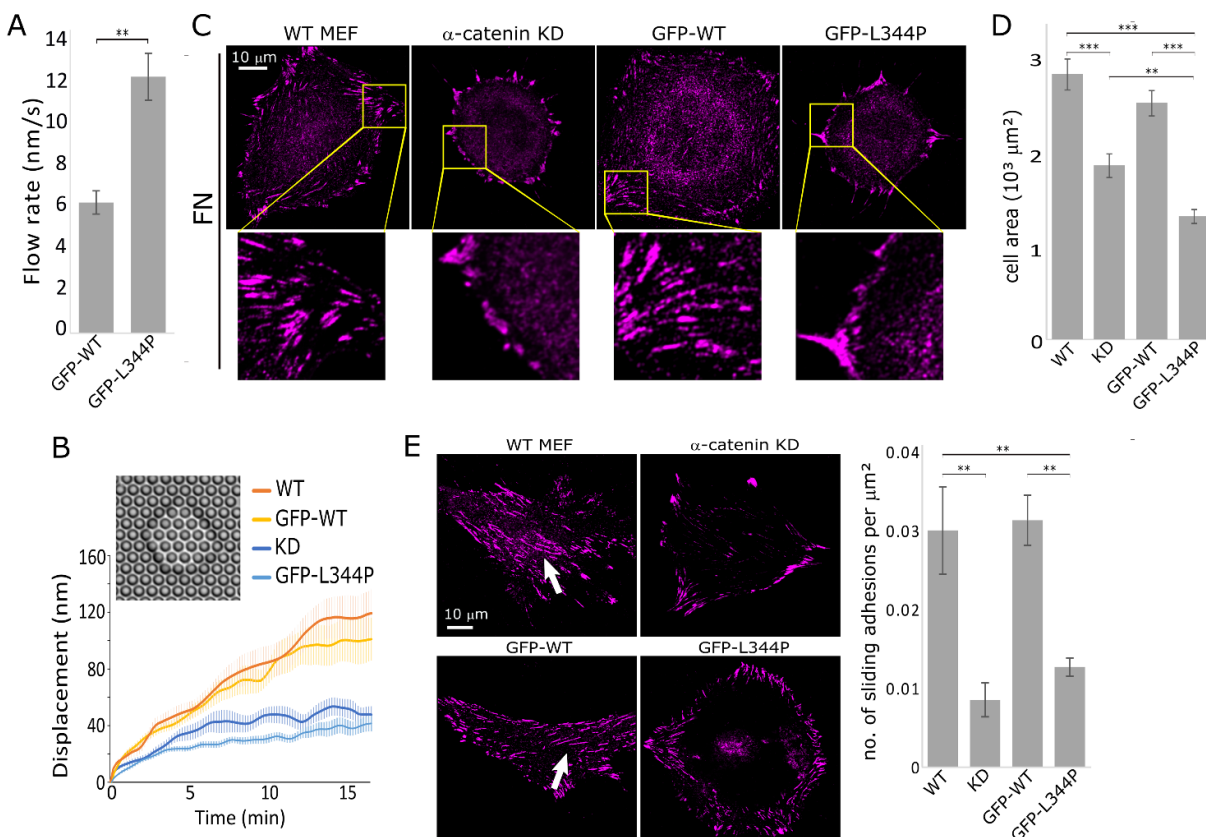


**Figure 4.  $\alpha$ -catenin L344P affects force transmission and adhesion maturation.** A. Flow rate of WT GFP- $\alpha$ -catenin and GFP- $\alpha$ -catenin L344P on top of integrin adhesions (N>15). B. Displacement as a function of time of 2 $\mu$ m diameter FN-coated pillars by cells spreading on top of them (see example in inset image). The graphs shown are mean  $\pm$  SEM (in lighter hues). N>30 pillars in each case. C. Immunostaining for vinculin and zoom-in on the cell edge of WT cells,  $\alpha$ -catenin KD cells, and  $\alpha$ -catenin KD cells expressing WT GFP- $\alpha$ -catenin or GFP- $\alpha$ -catenin L344P plated for 6 hours on FN-coated coverslips (GFP channel not shown). D. Mean cell area of the four cell types 6 hours after plating on FN-coated coverslips (N>50). E. Formation of sliding adhesions (arrows) on Matrigel-coated coverslips by WT cells,  $\alpha$ -catenin KD cells, and  $\alpha$ -catenin KD cells expressing WT GFP- $\alpha$ -catenin or GFP- $\alpha$ -catenin L344P (N>15 cells in each case). \*\*, P < 0.001; \*\*\*, P < 0.0001 (Student's t-test).

### $\alpha$ -catenin is not required for rigidity-dependent EMT but regulates rigidity-dependent growth following EMT

Since the  $\alpha$ -catenin–vinculin complex has a mechanosensory role within E-cadherin adhesions<sup>30</sup>, we next wanted to test whether it plays a similar role in the context of mechanosensing of ECM rigidity by integrin adhesions. Indeed, the observed decrease in matrix deformation upon the loss of  $\alpha$ -catenin–vinculin binding (Fig. 4B) suggests that this interaction is required for proper transmission of the contractile displacements involved in mechanosensing<sup>27</sup>. We first focused on the process of epithelial-to-mesenchymal transition (EMT), which was shown to occur on stiff matrices but not on soft ones<sup>31</sup>. We set out to test whether  $\alpha$ -catenin's dual role – in E-cadherin adhesions and in integrin adhesions – might be critical for this phenomenon, since cells that undergo EMT switch from relying on interactions with their neighboring cells to interactions with the matrix. Therefore, we used the epithelial Madin-Darby Canine Kidney (MDCK) cell line, as well as a variant of this cell line in which  $\alpha$ -catenin expression was knocked-down<sup>32</sup>. First, to test the effect of  $\alpha$ -catenin KD, we grew the cells for 48h on FN-coated glass coverslips, and then fixed and stained them for E-cadherin and vimentin – two markers whose expression levels are indicative of EMT (the former decreases while the latter



increases). WT MDCKs displayed a strong epithelial phenotype with tight E-cadherin connections between the cells and very low vimentin levels (Fig. 5A).  $\alpha$ -catenin KD MDCKs were less tightly packed compared to the WT cells, and still displayed E-cadherin adhesions, though this was accompanied with an increase in vimentin intensity (Fig. 5A), indicating that the cells had undergone partial EMT, in agreement with previous findings<sup>26</sup>. We next wished to test whether the absence of  $\alpha$ -catenin could affect the decision to undergo EMT as a function of matrix rigidity<sup>31</sup>. To that end, we plated both cell lines on soft (0.2kPa) and stiff (25kPa) FN-coated substrates for 3 hours before adding transforming growth factor beta (TGF $\beta$ ) to induce EMT. After a 48h incubation, WT cells remained epithelial on the soft matrix, as evident from the abundance of tight colonies with dominant E-cadherin staining in the borders between cells and low vimentin levels (Fig. 5B). On the stiff matrix, WT cells underwent partial EMT, as evident from the reduction in E-cadherin junctions, increased vimentin expression, and overall presence of isolated cells and cells that remained in somewhat loosely attached colonies (Fig. 5B, yellow arrows). KD cells on soft matrices were clustered in loosely attached colonies that did not display overall low E-cadherin levels but had weak E-cadherin junctions (Fig. 5B, second row, white arrows) which are indicative of them undergoing partial EMT (more advanced than the case of KD cells on glass without TGF $\beta$  treatment; compare the bottom row of Fig. 5A with the second row of Fig. 5B). On the stiff matrices, the KD cells underwent full EMT, as evident by the lack of cadherin junctions (accompanied by the presence of nuclear E-cadherin which is implicated in EMT<sup>33</sup>) and clear mesenchymal morphology with noticeable vimentin fibers extending throughout the cells (Fig. 5B). Thus, although the baseline phenotypes of WT and KD cells on soft matrices in the presence of TGF $\beta$  were different (fully epithelial and partial EMT, respectively), the stiff matrices shifted both cell types more toward the mesenchymal state (partial EMT and full EMT, respectively).

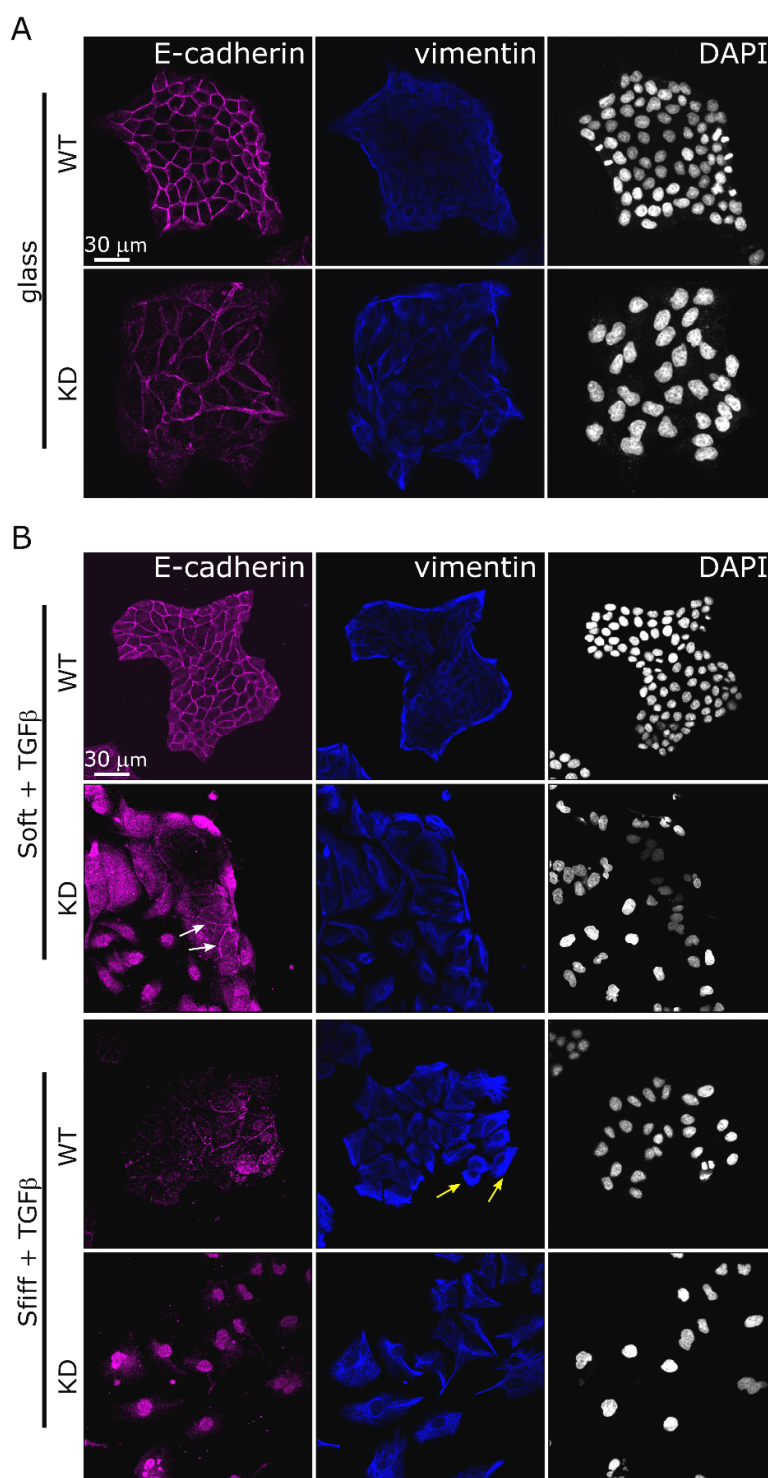


**Figure 5.  $\alpha$ -catenin does not affect rigidity-dependent EMT.** A. WT and  $\alpha$ -catenin KD MDCK cells stained for E-cadherin and vimentin after 48h on FN-coated glass without stimulation for EMT. B. WT and  $\alpha$ -catenin KD MDCK cells stained for E-cadherin and vimentin after 48h incubation with TGF $\beta$  (5ng/ml) on FN-coated soft (0.2kPa) and stiff (25kPa) matrices.

The results from the EMT assays suggest that the loss of  $\alpha$ -catenin does not affect rigidity-dependent EMT. However, we found that following EMT, WT cells displayed cell edge localization of  $\alpha$ -catenin. This was particularly noticeable in cells in which EGF was used to induce EMT (Fig. 6A). We therefore wanted to explore whether  $\alpha$ -catenin has a rigidity-dependent role in the mesenchymal state.  $\alpha$ -catenin was previously shown to be recruited to membranes rich with phosphatidylinositol-3,4,5-trisphosphate (PIP<sub>3</sub>) following EGF treatment<sup>20</sup>, and we previously found that EGF induces local rigidity sensing contractions at the cell edge on stiff but not soft matrices<sup>34</sup>. This led us to postulate that the cell edge recruitment of  $\alpha$ -catenin might also be rigidity-dependent. To test this, we plated WT MEFs on soft and stiff matrices, and then fixed and stained them for  $\alpha$ -catenin after 2.5, 5, 10, and 20 min exposure to EGF. This revealed that  $\alpha$ -catenin was recruited more rapidly and prominently to the cell edge on the stiff matrix compared to the soft one (Fig. 6B,C), thus reinforcing the idea that the regulatory role of  $\alpha$ -catenin might be most relevant in rigidity-dependent processes post EMT. Hence, we tested if  $\alpha$ -catenin affected the responses of mesenchymal cells to ECM rigidity. To that end, we plated WT and  $\alpha$ -catenin KD MEFs on 0.2kPa FN-coated surfaces, and tested their ability to survive and grow. 24h after plating, the vast majority of the WT cells had died and the remaining cells displayed clear apoptotic phenotypes (Fig. 6D). In contrast,  $\alpha$ -catenin KD MEFs were able to survive, spread, and proliferate (Fig. 6D). Notably, KD cells transfected with WT GFP- $\alpha$ -catenin displayed a similar phenotype as that of the WT MEFs, and KD cells transfected with GFP- $\alpha$ -catenin L344P were able to grow (Fig. 6D). Thus, the  $\alpha$ -catenin–vinculin link is required for proper responses to ECM rigidity. Moreover, when we induced EMT of WT and  $\alpha$ -catenin KD MDCK cells in plastic dishes and then transferred them onto soft FN-coated matrices, we found that the KD cells were able to survive and grow whereas the WT cells died within 24h (Fig. 6E). These results indicate the ability of  $\alpha$ -catenin to interact with vinculin is critical for cellular mechanosensing of ECM rigidity and regulates the anchorage-dependent growth of mesenchymal cells.

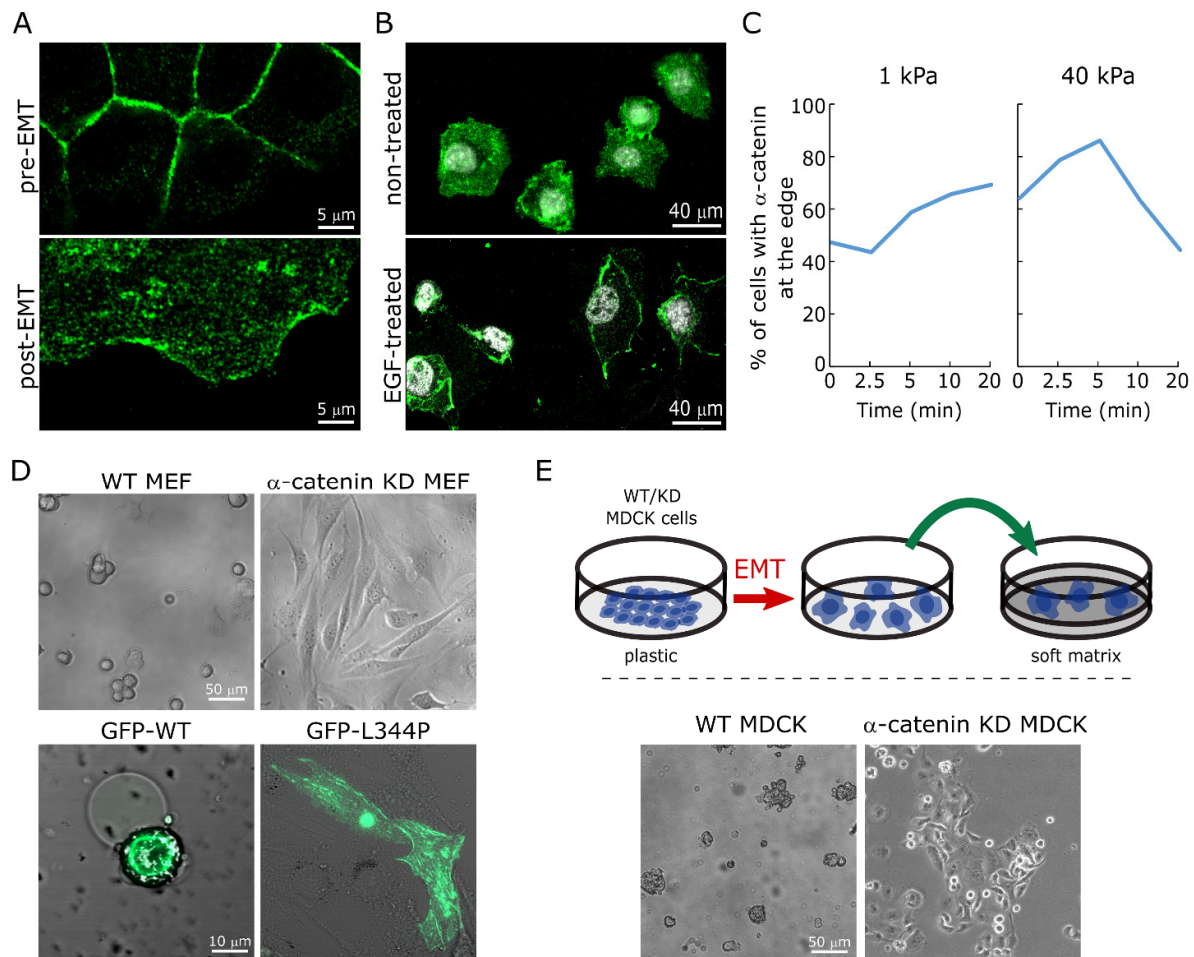


**Figure 6.  $\alpha$ -catenin controls rigidity-dependent cell growth at the mesenchymal state.** A.  $\alpha$ -catenin staining in WT MDCK cells before and after EMT (48h EGF treatment). B.  $\alpha$ -catenin staining in WT MEFs before and 5 min after EGF treatment. C. Quantification of the percentage of MEFs displaying  $\alpha$ -catenin edge localization as function of time after EGF addition ( $n > 100$  cells). D. WT MEFs,  $\alpha$ -catenin KD MEFs, and  $\alpha$ -catenin KD MEFs expressing WT GFP- $\alpha$ -catenin or GFP- $\alpha$ -catenin L344P plated for 24 hours on 0.2kPa FN-coated matrices. E. WT and  $\alpha$ -catenin KD MDCK cells post EMT plated for 24 hours on 0.2kPa FN-coated matrices.

## Discussion

In this study we identify a critical role for  $\alpha$ -catenin as a regulator of integrin adhesions and the associated actin cytoskeleton. We find that  $\alpha$ -catenin is recruited to lamellipodial regions, where it interacts with actin that is undergoing retrograde flow toward the cell center (Figs. 1&2). As actin travels past integrin adhesions along with  $\alpha$ -catenin, the latter interacts directly with vinculin in the adhesions (Fig. 3). This interaction is important for force transmission from the actin cytoskeleton through the adhesions, and, consistent with the concept of adhesion growth being a force-induced process, it is also important for the maturation of focal complexes into FAs (Fig. 4). At later stages,  $\alpha$ -catenin decorates stress fibers in regions devoid of  $\alpha$ -actinin, and the L344P mutant leads stress fibers to become highly contractile and aggregated at the cell center, suggesting that the  $\alpha$ -catenin–vinculin link affects stress fiber contractility. The underlying mechanism of this effect is not clear and should be addressed in future studies. One possibility is that the mere presence of  $\alpha$ -catenin enhances stress fiber contractility; hence, local/partial sequestration of  $\alpha$ -catenin by vinculin in the

adhesions would prevent excess  $\alpha$ -catenin translocation into the stress fibers, thereby attenuating excess contractility. Another possibility is that the poor connection between stress fibers and FAs in the presence of the L344P mutant limits the transmission of the contractile forces to the ECM, thereby leading to enhanced deformation of the stress fibers themselves, as predicted by our recent study<sup>27</sup>.

The classical model for the maturation of integrin adhesions involves the talin-vinculin module, and is described as a force-dependent mechanism in which talin stretching reveals hidden vinculin binding sites<sup>35</sup>. Thus, upon vinculin binding, the link between the cytoplasmic tails of the integrins and the actin cytoskeleton is reinforced, thereby stabilizing the adhesions<sup>36</sup>. Although the relevance of this model to the behavior of cells on soft and stiff matrices is still being debated<sup>37</sup>, the talin–vinculin module is clearly important for adhesion regulation and mechanosensing of the ECM. The results we present here provide an important addition to this picture with regards to the link between vinculin and actin. Although vinculin has an actin binding domain, it appears that its ability to bind to  $\alpha$ -catenin is in fact as, if not more important for proper interaction with F-actin, and consequently for proper force transmission and adhesion maturation. Moreover, we find that loss of  $\alpha$ -catenin–vinculin binding leads to impaired mechanosensing of matrix rigidity, which is manifested in the ability of mesenchymal cells to grow on soft matrices (anchorage-independent conditions) (Fig. 6). This falls in line with our previous observations which show that interfering with the rigidity sensing process could lead to transformed growth<sup>22,38,39</sup>.

Interestingly, we find that  $\alpha$ -catenin is not necessary for the decision to undergo rigidity-dependent EMT (Fig. 5). However, the role of  $\alpha$ -catenin in the process of EMT is not to be disregarded, as our results showed that the epithelial MDCK cell line undergoes (partial) EMT on soft surfaces upon treatment with TGF $\beta$  or EGF only when  $\alpha$ -catenin is absent from the cells. Notably, the absence of  $\alpha$ -catenin endows the cells the ability to grow on soft matrices after EMT, and thus  $\alpha$ -catenin KD cells can grow on both stiff and soft matrices when they are in the mesenchymal state. Thus, our results indicate that the tumor suppressor role of  $\alpha$ -catenin, which is typically attributed to its role in maintenance of AJs<sup>40</sup> and/or involvement in cytoplasmic sequestration of pro-proliferative transcriptional regulators<sup>21,41</sup>, should be re-evaluated given its role in regulating integrin adhesions. Particularly, the transformation of the cells to become anchorage-independent is a critical hallmark of cancer cells<sup>42</sup>, and the loss of  $\alpha$ -catenin–vinculin interaction appears to be crucial for this trait.



## **Materials and Methods**

### Cell culture, reagents, and transfections

WT MEFs (RPTP $\alpha^{+/+}$  cells), WT MDCK, and MDCK  $\alpha$ -catenin KD were received from MBI Singapore. MEF vinculin $^{-/-}$  cells were received from Benny Geiger's lab (Weizmann Institute of Science). All cells were cultured at 37° C in a 5% CO<sub>2</sub> incubator in Dulbecco's Modified Eagle Medium (DMEM) supplemented with 10% fetal bovine serum, and 100 IU/ml Penicillin-Streptomycin (all reagents were from Biological Industries). Recombinant human EGF (50 ng/ml), and TGF $\beta$  (5 ng/ml) were purchased from Peprotech (Rocky Hill, NJ). For EMT experiments, the cells were treated with EGF and TGF $\beta$  for 48-72 hours. For  $\alpha$ -catenin localization at the cell edge, the cells were allowed to spread overnight and then treated with EGF for a range of time points before fixation.

Transfections were carried out 1 day before measurements using the NEPA21 Electroporator (Nepa Gene) according to the manufacturer's instructions, with  $\sim 10^6$  cells per reaction and 10  $\mu$ g DNA.

### Plasmids and shRNA oligonucleotides

The WT GFP- $\alpha$ -catenin, GFP- $\alpha$ -actinin, GFP-vinculin, and Tomato-Tractin plasmids were obtained from MBI Singapore. The L344P mutation was inserted into the GFP- $\alpha$ -catenin plasmid using the Q5 Site-Directed Mutagenesis Kit (New England Biolabs).

Lentiviral KD of  $\alpha$ -catenin was performed using the SHCLNG-NM\_009818 MISSION® shRNA plasmid (Merck); control cells were generated using the SHC202 - MISSION® TRC2 pLKO.5-puro Non-Mammalian shRNA Control Plasmid (Merck). After infection, cells were grown in 4  $\mu$ g/ml puromycin, and KD was tested using Western blotting and immunofluorescence measurements.

### Pillars, soft gel fabrication, and cell spreading

Pillar fabrication was done by pouring PDMS (Sylgard 184, Dow Corning; mixing ratio – 10:1) into silicon molds (fabricated as previously described<sup>43</sup>) with holes at fixed depths and distances. The molds were then placed, face down, onto glass-bottom 35 mm dishes (#0 coverslip, Cellvis) which were incubated at 65°C for 12h to cure the PDMS. The molds were next peeled off while immersed in ethanol to prevent pillar collapse, which was then replaced by serial dilutions with PBS. Human plasma full-length fibronectin (Merck) was added to the dish at a final concentration of 10  $\mu$ g/ $\mu$ l for a 1h incubation at 37°C. Next, residual fibronectin was washed away by replacing the buffer to HBSS buffer (Biological Industries) supplemented with 20 mM HEPES (pH 7.2) or PBS.

All pillars had a diameter of 2  $\mu$ m, and heights of 9.4 or 13.2  $\mu$ m. We used 2  $\mu$ m diameter pillars as these can be used to measure the long-term time-dependent forces that are generated after initial formation and reinforcement of the adhesions<sup>38,43</sup>. The center-to-center spacing between pillars was 4  $\mu$ m. Pillar bending stiffness,  $k_{ECM}$ , was calculated by Euler–Bernoulli beam theory:

$$k_{ECM} = \frac{3\pi ED^4}{64 L^3}$$

where  $D$  and  $L$  are the diameter and length of the pillar, respectively, and  $E$  is the Young's modulus of the material ( $\approx 2$  MPa for the PDMS used here).

The 0.2 and 25kPa substrates were fabricated by using Sylgard 52-276, at a ratio of 2:1 and 1:2.7, respectively, according to the measurements performed by Ou et al.<sup>44</sup>.

#### Pillar displacement measurements

One day prior to the pillar experiments, cells were sparsely plated to minimize cell-cell interactions prior to re-plating. The following day, cells were trypsinized, centrifuged with growth medium, and then resuspended and pre-incubated in HBSS/Hepes at 37°C for 30 min prior to the experiment. Cells were then spread on the fibronectin-coated pillars. In all cases, we made sure that the cells were isolated when plated on the substrates.

Time-lapse imaging of cells spreading on the pillars was performed using an inverted microscope (Leica DMIRE2) at 37°C using a 63x 1.4 NA oil immersion objective. Brightfield images were recorded every 10 seconds with a Retiga EXi Fast 1394 CCD camera (QImaging). The microscope and camera were controlled by Micromanager software<sup>45</sup>. For each cell, a movie of 1-3 hours was recorded. To minimize photo-damage to the cells, a 600 nm longpass filter was inserted into the illumination path.

Tracking of pillar movements over time was performed with ImageJ (National Institutes of Health) using the Nanotracking plugin, as described previously<sup>38</sup>. In short, the cross-correlation between the pillar image in every frame of the movie and an image of the same pillar from the first frame of the movie was calculated, and the relative  $x$ - and  $y$ -position of the pillar in every frame of the movie was obtained. To consider only movements of pillar from their zero-position, we only analyzed pillars that at the start of the movie were not in contact with the cell and that during the movie the cell edge reached to them. Drift correction was performed using data from pillars far from any cell in each movie. For each pillar, the displacement curve was generated by Matlab (MathWorks).

#### Fluorescence microscopy

For immunofluorescence microscopy, cells were plated on fibronectin-coated coverslips or Matrigel-coated ibidi 8 well chamber slides, fixed with 4% paraformaldehyde supplemented with 0.2% Triton X-100. Immunolabeling was performed with primary antibodies against  $\alpha$ -catenin (Santa Cruz, sc-9988), vinculin (Thermo Fisher Scientific, #700062), E-cadherin (Merck, #U3254),  $\alpha$ -actinin (Abcam, #ab108198), and vimentin (Abcam, #ab24525) overnight at 4°C, and with Alexa Fluor 405, Alexa Fluor 488, Alexa Fluor 555, or Alexa Fluor 647-conjugated secondary antibodies. Images were taken with a Zeiss LSM800 confocal microscope using a 20x 0.9NA air objective or 63x 1.4NA oil objective.

#### EMT experiments

The MDCK WT and MDCK  $\alpha$ -catenin KD were sparsely plated on fibronectin coated 0.2 and 25 kPa PDMS gels. 3 hours after plating, EGF (50 ng/ml) or TGF $\beta$  (5 ng/ml) were added to the media and left for 48-72

hours before fixation and staining. In another set of experiments, the cells were made to undergo EMT and then plated on the 0.2kPa PDMS gels.

### Live cell imaging

The transfected cells were trypsinized, centrifuged with growth medium, and then resuspended and pre-incubated in HBSS/Hepes at 37°C for 5mins. These cells were then plated on fibronectin coated coverslips held in a ChamSlide CMS coverslip holder and live cell images were taken with a Zeiss LSM800 confocal microscope using a 63x 1.4NA objective at an interval of 20 seconds.

### Statistical analysis

All experiments were repeated at least twice on separate days using duplicates and triplicates on each day. Student's t-test was used to test the significance of difference between actin flow rates, number of adhesions, and cell area.

### Acknowledgments

H.W. acknowledges support from the Israel Science Foundation (1738/17) and from the Rappaport Family Foundation. H.W. is an incumbent of the David and Inez Myers Career Advancement Chair in Life Sciences. Author contributions: A.M. performed all the experiments and data analysis; E.N. performed cloning and assisted in generation of KD cell lines. M.P.S and H.W. conceived the idea for the studies. H.W. supervised the studies. A.M. and H.W. wrote the manuscript. Competing interests: The authors have no competing interests.

## References

1. Ringer, P., Colo, G., Fässler, R. & Grashoff, C. Sensing the mechano-chemical properties of the extracellular matrix. *Matrix Biology* **64**, 6–16 (2017).
2. Iskratsch, T., Wolfenson, H. & Sheetz, M. P. Appreciating force and shape—the rise of mechanotransduction in cell biology. *Nat. Rev. Mol. Cell Biol.* **15**, (2014).
3. Yap, A. S., Duszyc, K. & Viasnoff, V. Mechanosensing and mechanotransduction at cell – cell junctions. *Cold Spring Harb. Perspect. Biol.* **10**, a028761 (2018).
4. Maiden, S. L. & Hardin, J. The secret life of  $\alpha$ -catenin: moonlighting in morphogenesis. *J. Cell Biol.* **195**, 543–52 (2011).
5. Pokutta, S. & Weis, W. I. Structure and Mechanism of Cadherins and Catenins in Cell-Cell Contacts. *Annu. Rev. Cell Dev. Biol.* **23**, 237–261 (2007).
6. Sarpal, R. *et al.* Role of  $\alpha$ -Catenin and its mechanosensing properties in regulating Hippo/YAP-dependent tissue growth. *PLoS Genet.* **15**, (2019).
7. Yonemura, S., Wada, Y., Watanabe, T., Nagafuchi, A. & Shibata, M.  $\alpha$ -Catenin as a tension transducer that induces adherens junction development. *Nat. Cell Biol.* **12**, 533–542 (2010).
8. Thomas, W. A. *et al.*  $\alpha$ -Catenin and vinculin cooperate to promote high E-cadherin-based adhesion strength. *J. Biol. Chem.* **288**, 4957–4969 (2013).
9. Kobiela, A. & Fuchs, E.  $\alpha$ -catenin: At the junction of intercellular adhesion and actin dynamics. *Nature Reviews Molecular Cell Biology* **5**, 614–625 (2004).
10. Barry, A. K. *et al.*  $\alpha$ -Catenin cytomechanics - role in cadherin-dependent adhesion and mechanotransduction. *J. Cell Sci.* **127**, 1779–1791 (2014).
11. Buckley, C. D. *et al.* Cell adhesion. The minimal cadherin-catenin complex binds to actin filaments under force. *Science (80-. ).* **346**, 1254211 (2014).
12. Drees, F., Pokutta, S., Yamada, S., Nelson, W. J. & Weis, W. I.  $\alpha$ -Catenin Is a Molecular Switch that Binds E-Cadherin- $\beta$ -Catenin and Regulates Actin-Filament Assembly. doi:10.1016/j.cell.2005.09.021
13. Borghi, N., Lowndes, M., Maruthamuthu, V., Gardel, M. L. & Nelson, W. J. Regulation of cell motile behavior by crosstalk between cadherin- and integrin-mediated adhesions. *Proc. Natl. Acad. Sci. U. S. A.* **107**, 13324–13329 (2010).
14. Parsons, J. T., Horwitz, A. R. & Schwartz, M. A. Cell adhesion: Integrating cytoskeletal dynamics and cellular tension. *Nature Reviews Molecular Cell Biology* **11**, 633–643 (2010).

15. Wolfenson, H., Lavelin, I. & Geiger, B. Dynamic Regulation of the Structure and Functions of Integrin Adhesions. *Dev. Cell* **24**, 447–458 (2013).
16. Schwartz, M. A. Integrins and extracellular matrix in mechanotransduction. *Cold Spring Harb. Perspect. Biol.* **2**, a005066 (2010).
17. Weiss, E. E., Kroemker, M., Rüdiger, A. H., Jockusch, B. M. & Rüdiger, M. Vinculin is part of the cadherin-catenin junctional complex: Complex formation between  $\alpha$ -catenin and vinculin. *J. Cell Biol.* **141**, 755–764 (1998).
18. Sun, Y., Zhang, J. & Ma, L. alpha-catenin. A tumor suppressor beyond adherens junctions. *Cell Cycle* **13**, 2334–2339 (2014).
19. Vassilev, V., Platek, A., Hiver, S., Enomoto, H. & Takeichi, M. Catenins Steer Cell Migration via Stabilization of Front-Rear Polarity. *Dev. Cell* **43**, 463–479.e5 (2017).
20. Wood, M. N. *et al.*  $\alpha$ -Catenin homodimers are recruited to phosphoinositide-activated membranes to promote adhesion. *J. Cell Biol.* **216**, 3767–3783 (2017).
21. Piao, H. L. *et al.* alpha-catenin acts as a tumour suppressor in E-cadherin-negative basal-like breast cancer by inhibiting NF-kappaB signalling. *Nat. Cell Biol.* **16**, 245–254 (2014).
22. Meacci, G. *et al.*  $\alpha$ -Actinin links extracellular matrix rigidity-sensing contractile units with periodic cell-edge retractions. *Mol. Biol. Cell* **27**, (2016).
23. Roca-Cusachs, P. *et al.* Integrin-dependent force transmission to the extracellular matrix by alpha-actinin triggers adhesion maturation. *Proc. Natl. Acad. Sci. U. S. A.* **110**, E1361–70 (2013).
24. Belin, B. J., Goins, L. M. & Mullins, R. D. Comparative analysis of tools for live cell imaging of actin network architecture. *Bioarchitecture* **4**, 189–202 (2014).
25. Peng, X., Maiers, J. L., Choudhury, D., Craig, S. W. & DeMali, K. A.  $\alpha$ -Catenin uses a novel mechanism to activate vinculin. *J. Biol. Chem.* **287**, 7728–7737 (2012).
26. Seddiki, R. *et al.* Force-dependent binding of vinculin to  $\alpha$ -catenin regulates cell–cell contact stability and collective cell behavior. *Mol. Biol. Cell* **29**, 380–388 (2018).
27. Feld, L. *et al.* Cellular contractile forces are nonmechanosensitive. *Sci. Adv.* **6**, eaaz6997 (2020).
28. Zaidel-Bar, R., Ballestrem, C., Kam, Z. & Geiger, B. Early molecular events in the assembly of matrix adhesions at the leading edge of migrating cells. *J. Cell Sci.* **116**, 4605–4613 (2003).



29. Lu, J. *et al.* Basement Membrane Regulates Fibronectin Organization Using Sliding Focal Adhesions Driven by a Contractile Winch. *Dev. Cell* **52**, 631-646.e4 (2020).
30. Thomas, W. A. *et al.*  $\alpha$ -Catenin and vinculin cooperate to promote high E-cadherin-based adhesion strength. *J. Biol. Chem.* **288**, 4957–4969 (2013).
31. Wei, S. C. *et al.* Matrix stiffness drives epithelial-mesenchymal transition and tumour metastasis through a TWIST1-G3BP2 mechanotransduction pathway. *Nat. Cell Biol.* **17**, 678–688 (2015).
32. Benjamin, J. M. *et al.*  $\alpha$ E-catenin regulates actin dynamics independently of cadherin-mediated cell-cell adhesion. *J. Cell Biol.* **189**, 339–352 (2010).
33. Kolnes, A. J. *et al.* FSH Levels Are Related to E-cadherin Expression and Subcellular Location in Nonfunctioning Pituitary Tumors. *J. Clin. Endocrinol. Metab.* **105**, 2587–2594 (2020).
34. Saxena, M. *et al.* EGFR and HER2 activate rigidity sensing only on rigid matrices. *Nat. Mater.* **16**, 775–781 (2017).
35. del Rio, A. *et al.* Stretching single talin rod molecules activates vinculin binding. *Science* (80-. ). **323**, 638–641 (2009).
36. Elosegui-Artola, A. *et al.* Mechanical regulation of a molecular clutch defines force transmission and transduction in response to matrix rigidity. *Nat. Cell Biol.* **18**, 540–548 (2016).
37. Driscoll, T. P., Ahn, S. J., Huang, B., Kumar, A. & Schwartz, M. A. Actin flow-dependent and -independent force transmission through integrins. *Proc. Natl. Acad. Sci.* **117**, 202010292 (2020).
38. Wolfenson, H. *et al.* Tropomyosin controls sarcomere-like contractions for rigidity sensing and suppressing growth on soft matrices. *Nat. Cell Biol.* **18**, 33–42 (2016).
39. Yang, B. *et al.* Stopping transformed cancer cell growth by rigidity sensing. *Nat. Mater.* **19**, 239–250 (2019).
40. Bajpai, S., Feng, Y., Krishnamurthy, R., Longmore, G. D. & Wirtz, D. Loss of  $\alpha$ -catenin decreases the strength of single E-cadherin bonds between human cancer cells. *J. Biol. Chem.* **284**, 18252–18259 (2009).
41. Silvis, M. R. *et al.*  $\alpha$ -catenin is a tumor suppressor that controls cell accumulation by regulating the localization and activity of the transcriptional coactivator yap1. *Sci. Signal.* **4**, ra33–ra33 (2011).

42. Guadamillas, M. C., Cerezo, A. & Del Pozo, M. A. Overcoming anoikis--pathways to anchorage-independent growth in cancer. *J. Cell Sci.* **124**, 3189–3197 (2011).
43. Ghassemi, S. *et al.* Cells test substrate rigidity by local contractions on submicrometer pillars. *Proc. Natl. Acad. Sci. U. S. A.* **109**, 5328–5333 (2012).
44. Ou, G. *et al.* Visualizing mechanical modulation of nanoscale organization of cell-matrix adhesions. *Integr Biol* **8**, 795–804 (2016).
45. Edelstein, A., Amodaj, N., Hoover, K., Vale, R. & Stuurman, N. Computer control of microscopes using microManager. *Curr Protoc Mol Biol* **92** 14.20.1–14.20.17 (2010). doi:10.1002/0471142727.mb1420s92